Molecular Crystals and Liquid Crystals

ISSN: 1542-1406 (Print) 1563-5287 (Online) Journal homepage: https://www.tandfonline.com/loi/gmcl20

Effects of Operating Frequency on Panel-Aging and Discharge Characteristics in AC Plasma Display Panel

Choon-Sang Park , Jae Hyun Kim , Heung-Sik Tae , Bo-Sung Kim & Eun Young Jung

To cite this article: Choon-Sang Park , Jae Hyun Kim , Heung-Sik Tae , Bo-Sung Kim & Eun Young Jung (2013) Effects of Operating Frequency on Panel-Aging and Discharge Characteristics in AC Plasma Display Panel, Molecular Crystals and Liquid Crystals, 585:1, 41-49, DOI: 10.1080/15421406.2013.852882

To link to this article: https://doi.org/10.1080/15421406.2013.852882

Published online: 08 Jan 2014.

Mol. Cryst. Liq. Cryst., Vol. 585: pp. 41–49, 2013

ISSN: 1542-1406 print/1563-5287 online
DOI: 10.1080/15421406.2013.852882

Taylor & Francis
Taylor & Francis Group

Effects of Operating Frequency on Panel-Aging and Discharge Characteristics in AC Plasma Display Panel

CHOON-SANG PARK,[1] JAE HYUN KIM,[1] HEUNG-SIK TAE,[1,*] BO-SUNG KIM,[2] AND EUN YOUNG JUNG[3]

[1]School of Electronics Engineering, College of IT Engineering, Kyungpook National University, Daegu 702-701, Korea
[2]Display Nanomaterials Research Center, Kyungpook National University, Daegu 702-701, Korea
[3]Core Technology Lab., Corporate R&D Center, Samsung SDI Company Ltd., Cheonan, Chungcheongnam Do 330-300, Korea

This paper investigates the changes in the optical and discharge characteristics during the panel-aging process in ac plasma display panel as a parameter of the operating frequency. The resulting changes in the optical and discharge characteristics, including the firing voltage, dynamic voltage margin, three-dimensional IR emission, and SEM image, are then compared for the three different operating frequencies (10, 25, and 50 kHz) during the panel-aging process. Our experimental results confirm that the 50 kHz operating frequency is very effective in obtaining the uniform surface morphology of the MgO thin film during the panel-aging process.

Keywords Frequency; MgO thin film; panel aging; plasma discharge; plasma display panel; surface morphology

1. Introduction

Recently, to lower the panel fabrication cost, the PDP industry is focused on reducing the panel aging process time. The initial surface states of the MgO thin film prepared by the ion-plating method are very nonuniform and many impurities exist on the MgO surface. Accordingly, the panel-aging process is necessary to obtain the uniform MgO surface condition on both the ITO and bus electrodes for the stable discharge [1–6]. As such, the surface condition of the MgO layer on both the ITO and bus electrodes after the panel-aging process plays a decisive role in determining the initial discharge characteristics in an AC-PDP panel. One of the methods to reduce the panel-aging process time is simply to use the higher sustain voltage during the panel-aging process [7]. However, our previous experimental results show that the use of the higher sustain voltage during the panel-aging process results in the unstable discharge due to the occurrence of the self-erasing discharge

*Address correspondence to Prof. Heung-Sik Tae, School of Electronics Engineering, College of IT Engineering, Kyungpook National University, Sangyuk-dong, Buk-gu, Daegu 702-701, Korea (ROK). Tel.: (+82)53-950-6563; Fax: (+82)53-950-5505. E-mail: hstae@ee.knu.ac.kr

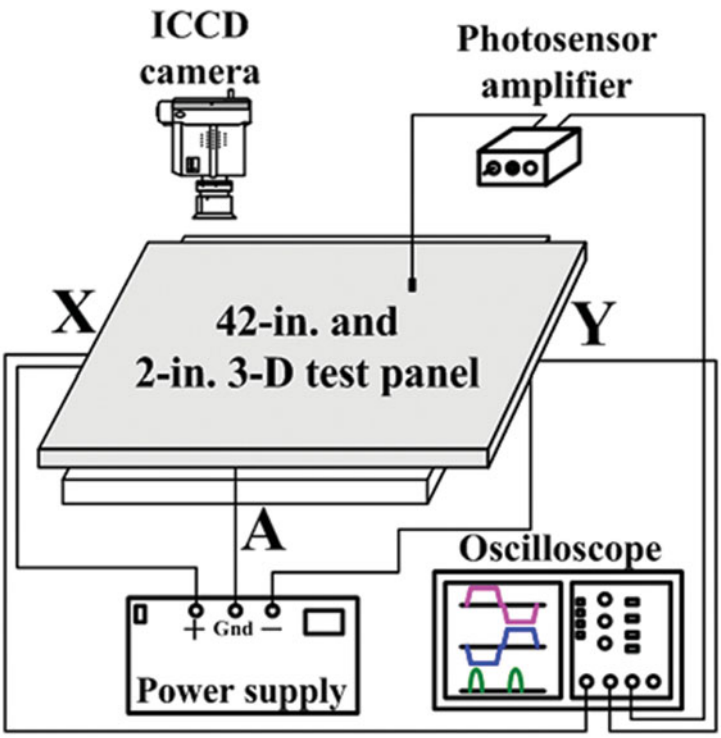

Figure 1. Schematic diagram of experimental setup employed in this study.

[7]. Many researches have so far reported the discharge characteristics under various driving frequencies during sustain driving period [8–10]. However, the influences of the operating frequency on the changes in the surface morphology of MgO layer in the display cell during the panel-aging process have not yet been studied systematically.

Accordingly, this paper examined the changes in the optical and discharge characteristics during the panel-aging process in ac plasma display panel as a parameter of the operating frequency in the 2- and 42-in. HD ac-PDP with He (35%)-Xe (11%) contents. In particular, the changes in the MgO surface morphology at a vicinity of the ITO and bus electrodes were examined under the three different operating frequencies (10, 25, and 50 kHz). Furthermore, the special 2-in. test panel was used to measure the 3-dimentional IR emission at the vicinity of the ITO and bus electrodes.

2. Simulation and Experimental Setup

Figure 1 shows the optical-measurement systems and 42-in. and 2-in. test panels with three electrodes, where X is the sustain-, Y the scan-, and A the address-electrode. A pattern generator, signal generator, ICCD camera, and photo-sensor amplifier (Hamamatsu, C6386) were used to measure the firing voltage, dynamic voltage margin, IR emission, and ICCD image, respectively. Figure 2 shows the single pixel structure of the 42-inch HD AC-PDP panel employed in this study. The indium tin oxide (ITO) electrode has a low conductivity, whereas the bus electrode made from Silver has a high conductivity. The gap between

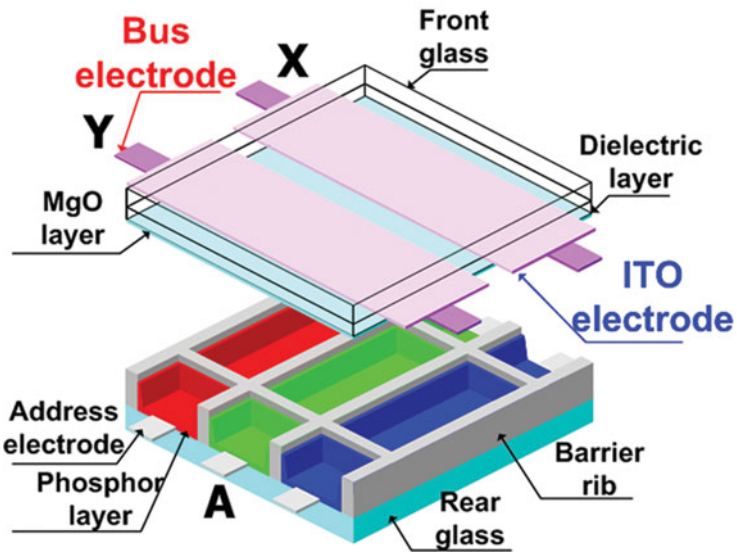

Figure 2. Schematic diagram of single pixel structure in 42-inch HD AC-PDP.

the two ITO electrodes is short, whereas the gap between the bus electrodes is long. The detailed panel specifications are listed in Table 1.

In this experiment, a 2-in. test panel was specially fabricated without phosphor layer only to investigate the three-dimensional IR emission during the plasma discharge in AC-PDP. Figure 3 shows the cross-sectional structure of the 2-in. test panel for observing three-dimensional IR emissions used in this study. The panel specifications of the 2-in. test panel in Fig. 3 were exactly the same with the 42-in. panel specifications in Fig. 2 and Table 1, except for the phosphor layer. In Fig. 3, to observe the side view of the plasma discharge in a unit cell, one flank of the closed wall was replaced by a polished glass prism, which was made of fused silica. The side images reflected by the glass prism were measured together with the top images [11].

Figure 4 shows the applied sustain driving waveform for the panel-aging process used in this study. The duty ratio and voltage for the sustain period was 40% and $\pm$150 V, respectively. The panel-aging process time was 5 hours. The different operating frequencies of driving waveforms were applied to the test panel during the aging process, as listed in Table 2.

Table 1. Specifications of 42-in. and 2-in. AC-PDP used in this study

Front Panel		Rear Panel	
ITO width	225 μm	Barrier rib width	55 μm
ITO gap	85 μm	Barrier rib height	120 μm
Bus width	50 μm	Address width	95 μm
Pixel pitch		912 μm $\times$ 693 μm	
Gas chemistry		Ne-Xe (11%)-He (35%)	
Gas pressure		430 Torr	

Table 2. Different operating frequencies applied to test panels during panel-aging process

	Case 1	Case 2	Case 3
Operating frequency	10 kHz	25 kHz	50 kHz

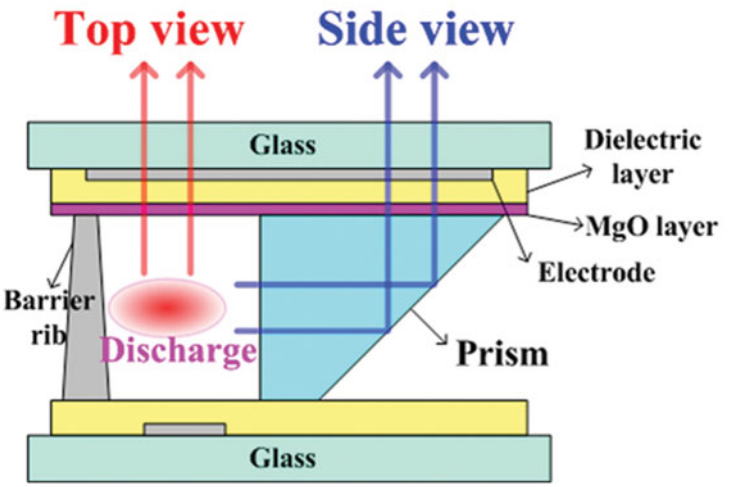

Figure 3. Schematic diagram of single pixel structure in 2-inch test panel having exactly same structure as 42-in. AC-PDP.

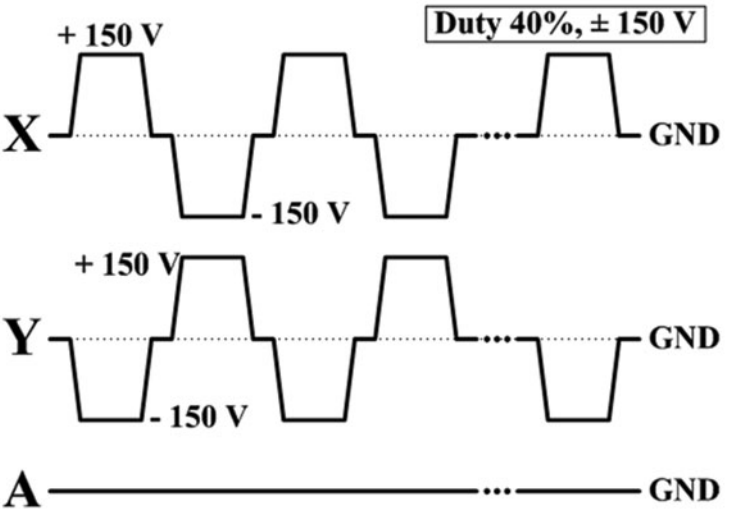

Figure 4. Schematic diagram of sustain driving waveform for panel-aging process used in this study.

Table 3. Comparison of discharge state detected by human eyes after 5 hour panel-aging process under various operating frequencies

	Discharge state after 5 h aging process
Case 1 (10 kHz)	Unstable
Case 2 (25 kHz)	Unstable
Case 3 (50 kHz)	Stable

3. Results and Discussion

3.1 Experimental Observation from 42-in. Test Panel

Aftr the 5 hour panel-aging process under the various operating frequencies, the discharge states are observed simply by the human eyes in Table 3. As shown in Table 3, for cases 1 and 2 (10 kHz and 25 kHz), the unstable discharge was produced after the panel-aging process. However, for case 3 (50 kHz), the stable discharges were produced after the panel-aging process.

Figure 5 shows the changes in the firing voltages during the panel-aging process for up to 5.5 hours on the 42-in. test panels under the various operating frequencies. As shown in Fig. 5, for all cases 1, 2, and 3, the firing voltages were stabilized in a short period of time after the 2 hour panel-aging process started.

Figure 6 shows the changes in the normalized dynamic voltage margins during the panel-aging process for up to 21 hours on the 42-in. test panels under the various operating frequencies. In Fig. 6, the normalized dynamic voltage margins was defined as the ratio of

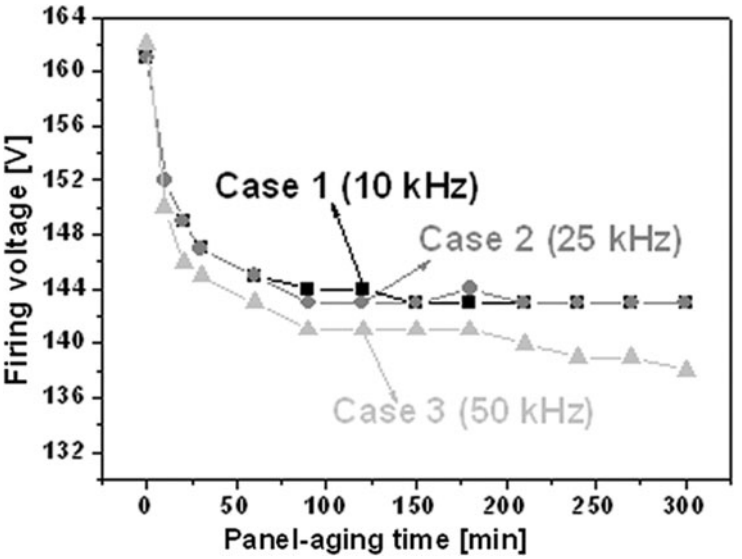

Figure 5. Comparison of firing voltages during panel-aging process measured from 42-in. HD test panels under various operating frequencies.

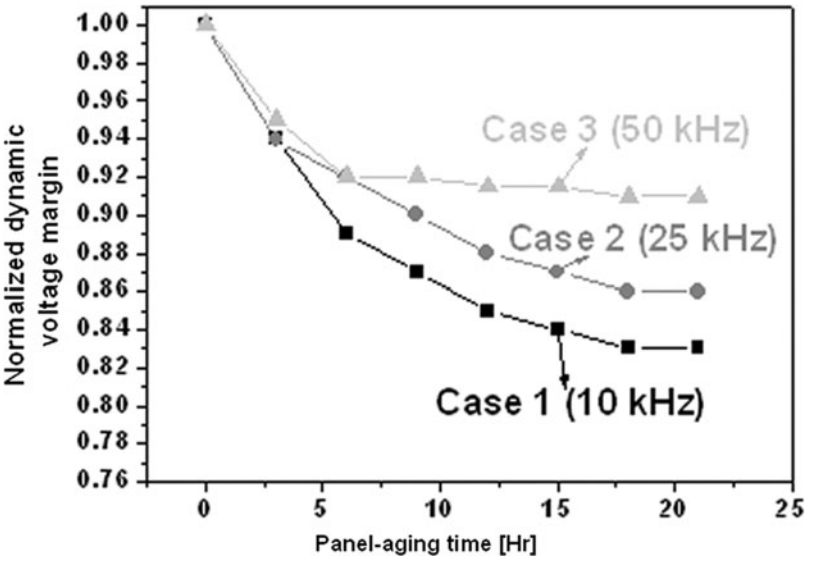

Figure 6. Comparison of normalized dynamic voltage margins during panel-aging process measured from 42-in. HD test panels under various operating frequencies.

the dynamic voltage margin difference between the initial voltage margin and the voltage margin with a panel-aging processing time. Thus, the normalized dynamic voltage margin of 1 corresponds to no difference of the dynamic voltage margin between the before and after panel-aging processes. As shown in Fig. 6, for cases 1 and 2, the normalized dynamic voltage margins were observed to be decreased continuously during the panel-aging time from the beginning of the measurement. However, for case 3, the normalized dynamic voltage margins were stabilized in a short period of time after the 5 hour panel-aging process started.

To investigate the reason for the stable discharge states after the panel-aging process under a higher (50 kHz) operating frequency, the SEM images were measured for the surface morphologies of the MgO thin film located on the ITO and bus electrodes.

Figure 7 shows the changes in the plane-SEM images of the MgO surfaces on the ITO and bus electrodes under the various operating frequencies in 42-in. test panels. As shown in Fig. 7, for cases 1 and 2, the MgO surface morphologies on the bus electrodes were observed to be larger than those on the ITO electrodes. However, for case 3, i.e., higher operating frequency case, the MgO surface morphologies for both ITO and bus electrodes were observed to be almost the same. We have reported that the continuous or more ion bombardment on the MgO thin film causes the surface morphology of the MgO thin film to get larger [6–8]. The surface morphologies shown in cases 1 and 2 of Fig. 7 mean that the MgO surface on the bus electrode was much more struck by the ions, compared to that on the ITO electrode, implying that the strong discharge was not spread towards the ITO electrode. On the other hand, for case 3, the MgO surface on both the ITO and bus electrodes was struck severely, implying that that the strong discharge was spread towards the end of the ITO electrode. Furthermore, the uniform MgO surface on both the ITO and bus electrodes can produce a stable discharge.

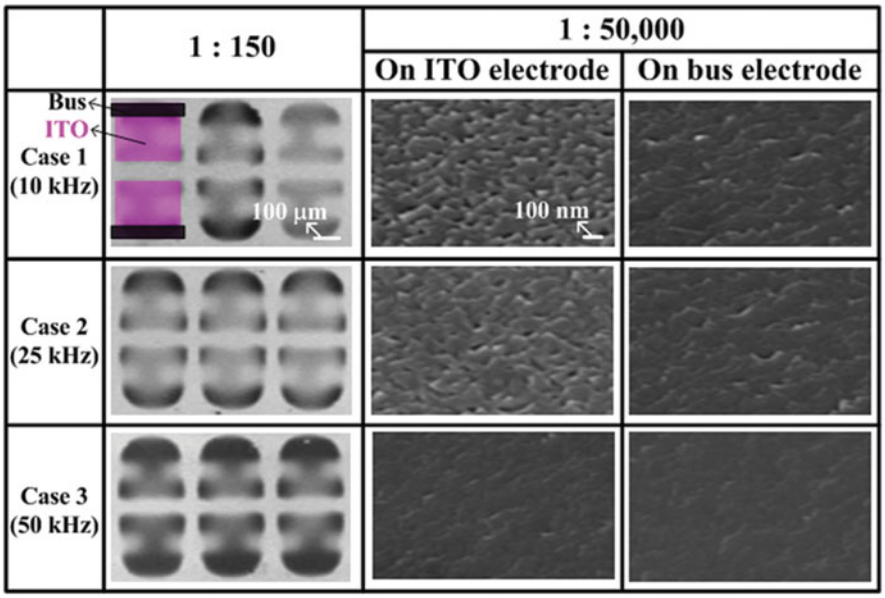

Figure 7. Comparison of SEM images of MgO surface changes on ITO and bus electrodes after 3 hour panel-aging process under various operating frequencies.

3.2 Experimental Observation of IR Emission from 2-in. Panel

To investigate the reason for obtaining the uniform MgO surface morphologies on both the ITO and bus electrodes after the panel-aging process under a higher operating frequency, the 2-in. test panel was fabricated to analyze the three-dimensional (3-D) spatiotemporal observations of the plasma discharge in PDP cell. The top and side discharge images were

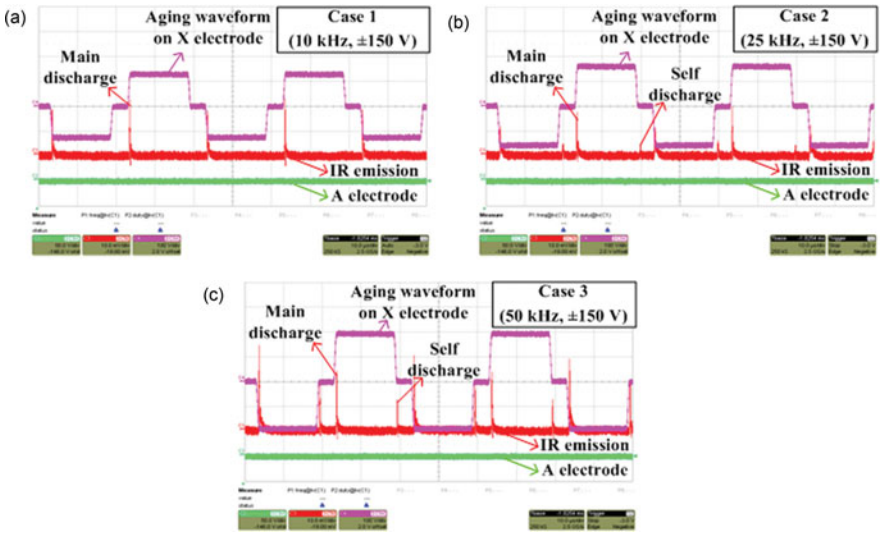

Figure 8. Comparison of IR emissions during-panel aging process under various operating frequencies. (a) Case 1 = 10 kHz, (b) Case 2 = 25 kHz, and (c) Case 3 = 50 kHz.

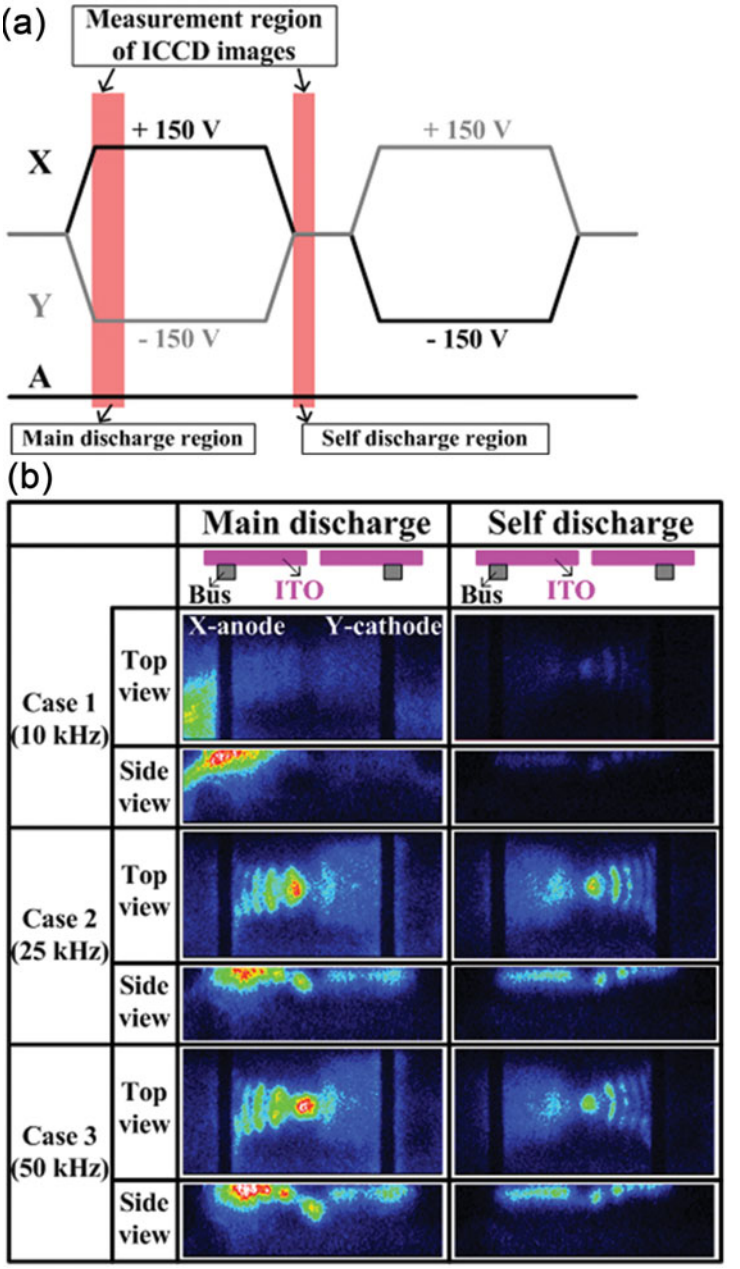

Figure 9. (a) Schematic diagram of sustain driving waveform identical to waveform in Fig. 4 and measurement point of ICCD images, and (b) comparison of top and side ICCD images during panel-aging process under various operating frequencies.

measured simultaneously by using the ICCD camera with the IR bandpass filter centered at 823 nm (10-nm bandwidth) [11].

Figure 8 shows the changes in the IR emissions during the panel-aging discharge under the various operating frequencies. Unlike case 1, the weak IR peak was observed with the strong peak for cases 2 and 3, as shown in Fig. 8, which indicated that the weak IR peak

emitted immediately after the falling of the sustain pulse was produced by the self-erasing discharge during the panel-aging process.

Figure 9(a) shows the ICCD measurement points for measuring the two discharges, i.e., the main discharge after the rising of the sustain pulse and the self-erasing discharge after the falling of the sustain pulse. Figure 9(b) shows the time-integrated top and side ICCD images of the main and self-erasing discharges. As shown in Fig. 9(b), from the side view of case 1, the discharge intensity on the bus electrode was stronger than that on the ITO electrode. In this case, i.e., case 1, the MgO surface morphologies for both ITO and bus electrodes were observed to be quite different, as shown in Fig. 7. However, from the side view of case 3, the discharge intensities were observed to be almost the same for both ITO and bus electrodes. In this case, i.e., case 3, the MgO surface morphologies for both ITO and bus electrodes were observed to be almost the same, as shown in Fig. 7. It is concluded that the higher operating frequency can stabilize the panel-aging discharge characteristics very fast by making the MgO surface morphologies on both the ITO and bus electrodes uniform.

Conclusion

In an AC-PDP manufacturing, the aging process is necessary to obtain a stable discharge. Accordingly, this paper examines the changes in the optical and discharge characteristics during the panel aging process in ac plasma display panel as a parameter of the operating frequency in the 42-in. HD ac-PDP with He (35%)-Xe (11%) contents. The resulting changes in the optical and discharge characteristics, including the firing voltage, voltage margin, three-dimensional IR emission, and SEM image, are then compared for various operating frequencies during the panel aging process. Our experimental results confirm that the high operating frequency is very effective in obtain the uniform surface morphology of the MgO thin film during the panel aging process. Under the high operating frequency condition, the MgO surfaces on both the ITO and bus electrodes are observed to be effectively aged, which is due to almost the same discharge intensities for both ITO and bus electrodes under the high operating frequency condition.

Acknowledgment

This research was supported by Basic Science Research Program through the National Research Foundation of Korea (NRF) funded by the Ministry of Education (2013R1A1A4A03008577).

References

[1] Choi, K. C., Kim, H.-J., & Shin, B. J. (2004). *IEEE Trans. Electron Devices*, *51*, 1241.
[2] Park, C.-S., & Tae, H.-S. (2010). *Appl. Phys. Lett.*, *96*, 043504.
[3] Park, C.-S., Tae, H.-S., Jung, E.-Y., Seo, J. H., & Shin, B. J. (2010). *IEEE Trans. Plasma Science*, *38*, 2439.
[4] Park, K.-H., Ko, M.-S, Yoon, S.-H., & Kim, Y.-S. (2007). *IMID'07 Dig.*, 216.
[5] Park, C.-S., & Tae, H.-S. (2009). *Applied Optics*, *48*, F78.
[6] Park, C.-S., Jang, S.-K., Tae, H.-S., & Jung, E.-Y. (2011). *Mol. Cryst. Liq. Cryst.*, *551*, 95.
[7] Park, C.-S., Tae, H.-S., Jung, E.-Y., & Ahn, J.-C. (2010). *Thin Solid Films*, *518*, 6153.
[8] Callegari, T., Boeuf, J.-P., Ouyang, J.-T., & Cao, J. (2004). *Chinese Physics B*, *13*, 1907.
[9] Kim, H., & Tae, H.-S. (2008). *IEEE Trans. Plasma Science*, *36*, 809.
[10] Li, Y.-M., Chen, C.-L., & Hsu, H.-B. (2003). *IEEE Trans. Electron Devices*, *50*, 913.
[11] Cho, T.-S., & Jung, J.-W. (2009). *IEEE Trans. Plasma Science*, *37*, 135.